

The Effect of Segmentation Variability in Forward ECG Simulation

Beata Ondrusova^{1,2}, Machteld Boonstra³, Jana Svehlikova¹, Dana Brooks⁴, Peter van Dam³,
Ali Salman Rababah⁵, Akil Narayan⁶, Rob MacLeod⁶, Nejib Zemzemi⁷, Jess Tate⁶

¹Institute of Measurement Science, Slovak Academy of Sciences, Bratislava, Slovakia

²Slovak University of Technology, Bratislava, Slovakia

³UMC Utrecht, Utrecht, The Netherlands

⁴Northeastern University College of Engineering, Boston, USA

⁵Royal Medical Services, Amman, Jordan

⁶University of Utah, Salt Lake City, USA

⁷Inria Bordeaux Sud Ouest, Bordeaux, France

Abstract

Segmentation of patient-specific anatomical models is one of the first steps in Electrocardiographic imaging (ECGI). However, the effect of segmentation variability on ECGI remains unexplored. In this study, we assess the effect of heart segmentation variability on ECG simulation. We generated a statistical shape model from segmentations of the same patient and generated 262 cardiac geometries to run in an ECG forward computation of body surface potentials (BSPs) using an equivalent dipole layer cardiac source model and 5 ventricular stimulation protocols. Variability between simulated BSPs for all models and protocols was assessed using Pearson's correlation coefficient (CC). Compared to the BSPs of the mean cardiac shape model, the lowest variability (average $CC = 0.98 \pm 0.03$) was found for apical pacing whereas the highest variability (average $CC = 0.90 \pm 0.23$) was found for right ventricular free wall pacing. Furthermore, low amplitude BSPs show a larger variation in QRS morphology compared to high amplitude signals. The results indicate that the uncertainty in cardiac shape has a significant impact on ECGI.

1. Introduction

Electrocardiographic imaging (ECGI) is of interest to guide clinical diagnosis, treatment and risk-stratification in patients. In ECGI, body surface potential (BSP) measurements are combined with patient-specific anatomical models to estimate cardiac electrical activity. Mathematical models are established to relate cardiac electrical activity to BSPs [1]. Whereas it is known that ECGI estimations are affected by the parameter settings in this forward model [2], many questions remain on the effect of segmentation uncertainty. It was shown

previously that segmentations differ mainly for cardiac geometry [3]. Thus, in the research presented in this paper, we focus to study the variation in segmentation that may significantly affect computed BSPs from equivalent dipole layer source models. The study builds on previous research that was conducted by the Consortium for ECG Imaging (CEI) (<https://www.ecg-imaging.org/>) [3,4].

2. Materials and Methods

To describe the effect of variation in segmentations on computed BSPs, we implemented a statistical shape model derived from 15 ventricular segmentations of a single patient. Subsequently we simulated multiple BSPs, and computed statistics on the BSPs to relate to the shape statistics (Figure 1). The CT scans used in this study are publicly available on the EDGAR database as the Dalhousie dataset (<https://www.ecg-imaging.org/edgar-database>) [5].

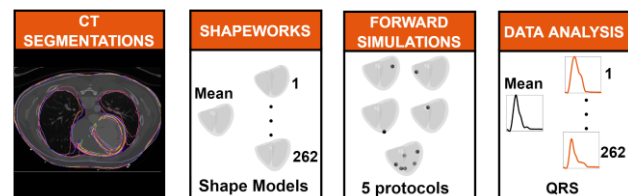


Figure 1. Study pipeline.

2.1. Statistical Shape Model

The statistical shape model used in this study was computed using ShapeWorks [6] on the 15 cardiac segmentations that were prepared by 15 different observers using their own in-house software tools. ShapeWorks contains a particle system optimizer that computes

correspondence points between all segmentations allowing to compute statistical shape models. The generated shape model comprises the mean shape and the major modes of variation computed using principal component analysis (PCA). The first five shape modes (Figure 2) capture >90% of the shape variability and were included in the shape model. The shape model was sampled 262 times using weighted Fekete sampling [7] assuming a uniform distribution along each shape mode and a range of 2 times the computed standard deviation (σ) computed for each axis. The correspondence points derived from these samples were used to generate closed triangulated surface meshes for forward simulation and for comparison of cardiac data between samples.

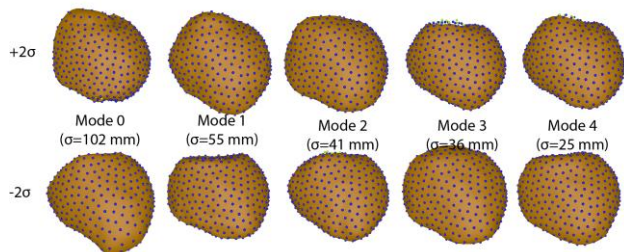


Figure 2. First five modes of variation with standard deviation (σ) presented in mm.

2.2. Forward Simulations

For all generated cardiac meshes, five types of ventricular stimulation protocols were used, consisting of four paced beats and one sinus beat (Figure 3). The paced beats were initiated in the left ventricle free wall, right ventricle free wall, at the apex or the septum whereas the sinus beat was represented with six simultaneous foci to mimic healthy ventricular activation. Ventricular activation sequences were calculated using the fastest route algorithm [8] assuming uniform propagation velocity (1.15 m/s) for each shape model and stimulation protocol. Subsequently, BSPs were computed using the equivalent dipole layer (EDL) cardiac source model [2] with the boundary element method-based volume conductor model. Local source strength was determined by the local transmembrane potential (TMP) shape. The BSPs were computed for all cardiac shapes assuming the same homogeneous torso model with 120 electrodes.

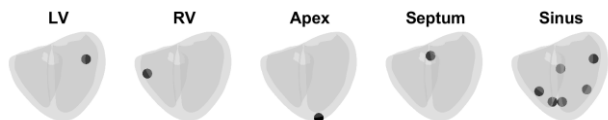


Figure 3. Ventricular stimulation protocols depicted for the mean cardiac shape model.

2.3. Data Analysis

For all BSPs simulations, all parameters were kept

constant to specifically study the effect of the cardiac shape on the depolarization phase in computed BSPs. Analysis was focused on local activation timing (LAT) maps at correspondence points and the simulated QRS complexes. LAT at correspondence points was computed per shape model using linear interpolation. Simulated BSPs were compared by means of correlation coefficient (CC), QRS duration and RS amplitude. Root mean square (RMS) signals were computed for the 120-lead BSPs per model for each simulation. Per time instant, the variation in the RMS signal was determined by dividing the range in the amplitude of the RMS signal by the mean of the amplitude at the same time instance. Data are presented as mean \pm standard deviation or median [range] as appropriate.

3. Results

Compared to the LAT sequence of the mean shape model, the average CC was 0.98 ± 0.02 and the average absolute difference in LAT was 2.8 ± 3.2 ms. For all stimulation protocols, the standard deviation in LAT ranged between 0 and 22 ms (Table 1).

Table 1. Average correlation coefficient (CC_{avg}), average absolute difference (AD_{avg}), and standard deviation range ($STDev_r$) in local activation timing (LAT) for all protocols.

Protocol	CC_{avg} [-]	AD_{avg} [ms]	$STDev_r$ [ms]
LV	0.99 ± 0.01	4 ± 9	0 - 11
RV	0.98 ± 0.02	5 ± 9	0 - 22
Apex	0.99 ± 0.01	4 ± 12	0 - 8
Septum	0.97 ± 0.04	3 ± 7	0 - 20
Sinus	0.98 ± 0.01	3 ± 6	0 - 7

The variability in computed QRS complex for the five protocols is shown in Figure 4 for two representative leads of the standard 12-lead ECG. The simulated BSPs differ in both morphology and QRS duration. On model-to-model basis, the lowest average CC 0.54 ± 0.40 was observed for lead V1 when simulating septal stimulation (Figure 5).

The average CC between QRS complexes was 0.93 ± 0.07 over all stimulation protocols. Compared to the QRS complex of the mean shape model, the average CC was 0.95 ± 0.13 (Table 2). Between stimulation protocols, there were small differences. The highest average CC was observed for the stimulation protocol initiated at the apex of the ventricles, whereas the lowest average CC was observed for the RV paced beat. The average QRS duration was the highest for RV stimulation, but the highest standard deviation with respect to the average QRS duration was observed for the LV stimulation protocol (Table 2).

The variation in RMS signals (Figure 6) showed that for all beats, the variation was highest at end of the QRS complex. But whereas the variation differed for LV, RV, and septal stimulation over the course of the QRS complex,

for apical stimulation it remained similar.

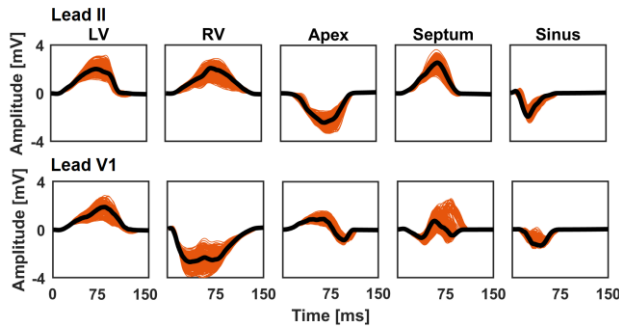


Figure 4. The simulated QRS complexes for all 262 cardiac shape models (orange) and mean shape (black) for a lead II and V1 of a standard 12-lead ECG for all protocols.

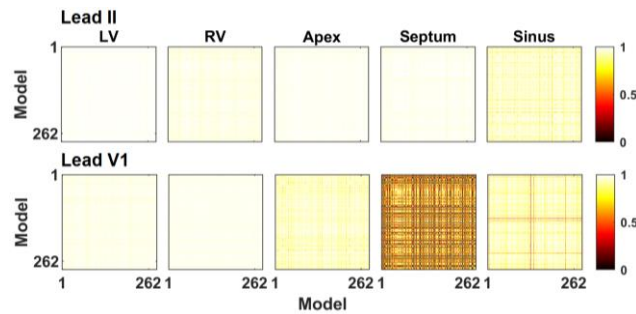


Figure 5. Pearson's correlation matrix for a lead II and V1 of a standard 12-lead ECG for all protocols.

Table 2. Average correlation coefficient (CC_{avg}), the range of CC (CC_r) and QRS duration (QRSdur) for all protocols.

Protocol	CC_{avg} [-]	CC_r [-]	QRSdur [ms]
LV	0.97 ± 0.10	-0.86 – 1.00	124.14 ± 5.35
RV	0.90 ± 0.23	-0.86 – 1.00	134.69 ± 3.87
Apex	0.98 ± 0.03	0.50 – 1.00	114.75 ± 2.40
Septum	0.95 ± 0.11	-0.63 – 1.00	98.04 ± 3.44
Sinus	0.93 ± 0.10	-0.62 – 1.00	70.26 ± 2.68

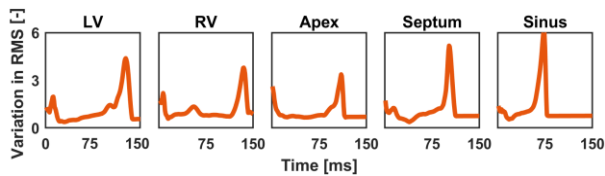


Figure 6. The variation in RMS signal for all protocols.

Per stimulation protocol, the torso electrodes most affected by the variation in cardiac shape were different (Figure 7). In the stimulation protocol with the highest average CC (Table 2, apex), variation in CC over all electrodes was low whereas with lower average CC, variation over electrodes in CC was higher. The variation in QRS complexes for the five electrodes with the lowest average CC for RV stimulation shows that the RS amplitude ratio of the QRS changes and the amplitude of the QRS complexes is low for those signals (Figure 8). There was a relation between RS amplitude and CC, with

lower CCs QRS complexes had lower amplitude (Figure 9) for all stimulation protocols.

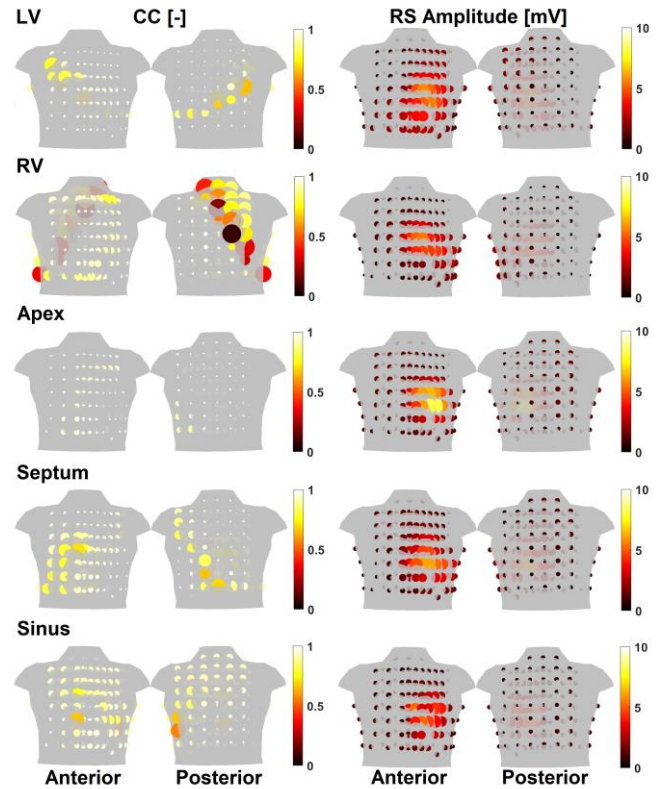


Figure 7. The average CC and RS amplitude computed for all torso electrodes and all protocols for the anterior and posterior sides of the torso. The color of the electrode corresponds to the average CC or RS amplitude computed per electrode for all shape models and the size of the electrode increases with increasing standard deviation.

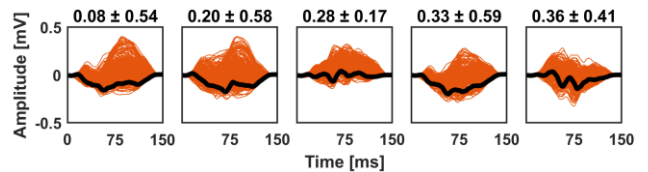


Figure 8. The simulated QRS complexes for all 262 cardiac shape models (orange) and mean shape (black) for selected torso electrodes with the lowest mean CC for RV stimulation protocol.

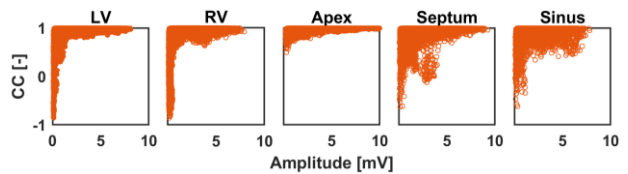


Figure 9. The CCs vs RS amplitude for all cardiac shape models and all protocols.

4. Discussion

In this study, we analyze the effect of variability in cardiac segmentations on the solution of the forward problem. An overall good correlation (0.98 ± 0.02) was observed between LAT sequences per stimulation protocol (Table 1). We demonstrate that BSPs computed for 262 cardiac shape models vary on both the model-to-model (Figure 5) and model-to-mean basis (Figures 4, 7 and 8). Per stimulation protocol, different leads were affected most (Figure 7). The lowest CC values were observed with RV pacing and the highest for apical pacing (Table 2). When relating this to the cardiac segmentation variability [3], the lowest variability in shape was also observed around the apex of the heart. Thus, the lower variability in QRS morphology may be the result of an overall more similar average direction (apex to base) of activation waves traveling through the heart during apical pacing when compared to the other paced beats. For apical stimulation, the variation in the basal segment is likely to significantly change QRS morphology only at the beginning and end of the QRS complex, but less effect is expected in mid-QRS as the main direction of cardiac activation remains similar from apex to base (Figure 6). In the other pacing protocols, changes at mid-QRS are observed, which can be explained by the fact that if the pacing sites are closer to the base it will thus affect QRS morphology at mid-QRS, as the basal region is activated earlier.

Furthermore, we showed that simulated QRS complexes for all torso electrodes were not equally affected by the variation in cardiac shape and that some electrodes show higher differences amongst simulated QRS complexes also depending on the pacing site. Higher differences between simulated QRS complexes occurred near the base of the heart, corresponding to high shape variability [3]. The highest differences in computed BSPs in terms of the CC were observed on the posterior side of the torso during RV pacing [3]. Signals in this area also showed low amplitude, however not all low amplitude signals had low CC (Figure 7). The high variability of the CC in the posterior region denotes that it is an area where the direction of activation changes the most.

The results of this study suggest that the variation in cardiac shape affects the simulated BSPs. However, a more comprehensive study needs to be done to further quantify how the variation in shape affects the solution of the forward problem and consequently the ECGI estimation of cardiac activity. Furthermore, we used a simple model to simulate the activation sequences and did not yet focus on the repolarization phase. The effect of the application of repolarization gradients and more sophisticated models of cardiac activation will also be assessed with regards of the uncertainty quantification.

5. Conclusion

In this study, we showed that a high variation in shape is observed at the base of the ventricles around the heart valves. It was shown that this variation in cardiac shape affects the simulated BSPs. The extent to which the simulated signals are affected depends on the ventricular stimulation protocol used. The results suggest that variation in cardiac shape may have a significant impact on the ECGI. Thus, more emphasis must be placed on the study of the effects of variability in segmentations on the accuracy of the ECGI which plays an important role in clinical practice.

Acknowledgments

This work was supported by the VEGA Grant Agency in Slovakia under grant number 2/0109/22, by the Slovak Research and Development Agency under grant number APVV-19-0531, by the National Institutes of Health under grant number NIBIB-U24EB029011. The authors would like to thank all who generously provided the segmentations used in this study.

References

- [1] R. M. Gulrajani, "The forward and inverse problems of electrocardiography," *IEEE eng. med. biol. mag.*, vol. 17, no. 5, pp. 84–101, Sept.-Oct. 1998.
- [2] P.M. van Dam, "ECGSIM: interactive simulation of the ECG for teaching and research purposes", *2010 CinC*, pp. 841-844, Sept 2010.
- [3] J. D. Tate et al., "A Cardiac Shape Model for Segmentation Uncertainty Quantification", *2021 CinC*, vol. 48, pp. 1-4, Sept. 2021.
- [4] J. D. Tate, "Uncertainty quantification of the effects of segmentation variability in ECGI", *FIMH 2021*, vol. 12738, pp. 515-522, June 2021.
- [5] J. L. Sapp, F. Dawoud, J. C. Clements, B. M Horacek, "Inverse solution mapping of epicardial potentials: quantitative comparison with epicardial contact mapping", *Circ Arrhythm Electrophysiol*, vol. 5, pp. 1001-1009, Oct. 2012.
- [6] J. Cates, S. Elhabian, R. Whitaker, "Shapeworks: particle-based shape correspondence and visualization software", *Statistical Shape and Deformation Analysis*. Academic Press, pp. 257-298, 2017.
- [7] K.M Burk, A. Narayan, J.A. Orr, "Efficient sampling for polynomial chaos-based uncertainty quantification and sensitivity analysis using weighted approximate feket points", *Int J Numer Meth Biomed Eng.*, vol. 36(11), pp. 1-25, Nov.2020.
- [8] P. M. van Dam, T. F. Oostendorp, A. van Oosterom, "Application of the fastest route algorithm in the interactive simulation of the effect of local ischemia on the ECG", *Med. Biol. Eng. Comput.*, vol. 47, no. 1, pp. 11-20, Sept. 2009.

Address for correspondence:

Beata Ondrusova
Institute of Measurement Science, Slovak Academy of Sciences
Dubravska cesta 9, 841 04, Bratislava, Slovakia
beata.ondrusova@savba.sk